Published in final edited form as:
Int J Hyperthermia. 2013 December ; 29(8): 835–844. doi:10.3109/02656736.2013.834384.

Magnetic Fluid Hyperthermia for Bladder Cancer: A Preclinical Dosimetry Study

Tiago R. Oliveira[1,2], **Paul R. Stauffer**[*,1], **Chen-Ting Lee**[1], **Chelsea D. Landon**[1], **Wiguins Etienne**[3], **Kathleen A. Ashcraft**[1], **Katie L. McNerny**[4], **Alireza Mashal**[4], **John Nouls**[5], **Paolo F. Maccarini**[1], **Wayne F. Beyer Jr.**[6,7], **Brant Inman**[3], and **Mark W. Dewhirst**[1]

[1]Department of Radiation Oncology, Duke University Medical Center, Durham, NC, 27710

[2]Instituto de Física, Universidade de São Paulo, São Paulo, Brazil, 05508-090

[3]Division of Urology, Duke University Medical Center, Durham, NC 27710

[4]Actium Biosystems, Boulder, CO 80301

[5]Center for In Vivo Microscopy, Duke University Medical Center, Durham, NC 27710

[6]QNS Group, LLC, Bahama, NC 27503

[7]Duke Translational Research Institute, Duke University Medical Center, Durham NC 27710

Abstract

Purpose—This paper describes a preclinical investigation of the feasibility of thermotherapy treatment of bladder cancer with Magnetic Fluid Hyperthermia (MFH), performed by analyzing the thermal dosimetry of nanoparticle heating in a rat bladder model.

Materials and Methods—The bladders of twenty-five female rats were instilled with magnetite-based nanoparticles, and hyperthermia was induced using a novel small animal magnetic field applicator (Actium Biosystems, Boulder, CO). We aimed to increase the bladder lumen temperature to 42°C in <10 min and maintain that temperature for 60 min. Temperatures were measured within the bladder lumen and throughout the rat with seven fiberoptic probes (OpSens Technologies, Quebec, Canada). An MRI analysis was used to confirm the effectiveness of the catheterization method to deliver and maintain various nanoparticle volumes within the bladder. Thermal dosimetry measurements recorded the temperature rise of rat tissues for a variety of nanoparticle exposure conditions.

Results—Thermal dosimetry data demonstrated our ability to raise and control the temperature of rat bladder lumen ≥1°C/min to a steady-state of 42°C with minimal heating of surrounding normal tissues. MRI scans confirmed the homogenous nanoparticle distribution throughout the bladder.

Conclusion—These data demonstrate that our MFH system with magnetite-based nanoparticles provide well-localized heating of rat bladder lumen with effective control of temperature in the bladder and minimal heating of surrounding tissues.

[*]paul.stauffer@duke.edu; phone: 919-668-7419.

Keywords

bladder cancer; hyperthermia; nanoparticle heating; iron oxide; thermal dosimetry

INTRODUCTION

Numerous reports have established that combining local or regional hyperthermia (HT) with chemotherapy improves treatment outcomes for solid tumors [1–3]. Mild hyperthermia, which raises the local temperature to approximately 42°C, can promote additional drug uptake in tumor tissue due to increased blood flow and vascular permeability. For clinical thermal therapy applications, precise control of temperature in and around the target volume is a crucial factor in therapeutic outcome. Effective control of temperature relies on the ability of the heat source to adapt to unique characteristics of both the target tissue and the surrounding environment. Currently, one of the major challenges for hyperthermia is establishing techniques that treat deep-seated organs, such as bladder, with effective localization of power deposition and without overheating the surrounding normal tissues.

Urothelial carcinomas account for approximately 90% of all bladder cancers [4]. This disease originates in cells lining the inside of the bladder wall and presents as either non-muscle invasive (NMIBC) or muscle invasive bladder cancer (MIBC) [5]. For NMIBC, the initial therapy strategy of transurethral resection of the bladder tumor (TURBT) is associated with a high local recurrence rate of 40–80%, potentially leading to additional surgeries and subsequent treatments [6, 7]. The high recurrence rate has motivated the search for more efficacious therapeutic approaches such as thermochemotherapy. Attempts to use hyperthermia for treating bladder cancer have been reported previously [8, 9]. However, the inability to effectively monitor and control the delivery of heat to the bladder has significantly delayed use of hyperthermia in this site. The recent evolution of hyperthermia delivery capabilities has rekindled interest in hyperthermia as an adjuvant treatment for bladder cancer. To date, most clinical studies using hyperthermia for the treatment of bladder cancer have used a miniature 915 MHz microwave antenna (Synergo SB-TS System) inserted into the bladder to heat urine and drug inside the bladder [10]. The challenges for effective treatment are to achieve homogenous therapeutic temperatures at all points along the bladder wall, and to maintain the minimum temperature for the duration of treatment without excessive heating of surrounding normal tissues. The Synergo heating approach has provided promising clinical results; however, with the highly localized power delivery and limited control of antenna position within the bladder lumen, side effects such as pelvic pain and bladder wall injury also resulted from use of this system [10–13]. Alternative methodologies are under investigation for heating bladders filled with the chemotherapeutic agent Mitomycin-C using radiofrequency (RF) capacitive electrodes [14, 15] or RF phased array applicators [16] to heat a larger region of the pelvis including bladder. Additionally, recent preclinical investigations have demonstrated effective bladder heating of small animals with water-cooled external microwave applicators [17].

Over the past fifteen years, there has been a substantial focus placed on investigating the underlying principles and clinical feasibility of Magnetic Fluid Hyperthermia (MFH). MFH

heats the desired target region by coupling energy from an external alternating magnetic field into magnetic nanoparticles (MNP), following their injection into the target tissue. Although numerous MFH studies exist in the current literature, only a few have progressed to clinical trials. Most clinical experience to date has involved the Nanoactivator system (Magforce AG, Berlin, Germany) used in feasibility studies in patients with recurrences of glioblastoma multiforme [18, 19] and prostate cancer [20, 21]. Based on these studies, the main limitations included difficulties in dispersing MNP homogeneously throughout the tumor tissue, and patient discomfort at high magnetic field strengths.

The application of MFH for urinary bladder cancer has several potential advantages over other organ targets and heating approaches. First, MFH heating is restricted to anatomical regions with both high magnetic field strength and high concentration of magnetic material. In the case of bladder, magnetic particles are easily concentrated within the bladder by direct injection of magnetic nanoparticles. Using one of several different induction coil types, relatively uniform magnetic fields may be produced deep in the body that cause minimal direct heating of tissue [22–24]. The ease of urinary catheterization facilitates direct intravesical installation of magnetic particles to the bladder target, which can be easily concentrated by modulating the instillation quantity/volume. The structure of the intravesical space allows the injected solution to remain in contact with the tumor tissue (bladder wall) without significant interaction with other normal tissues at a distance from the bladder. The urothelium, which consists of a thick layer of epithelial cells with tight junctions (uroplakin), covered by a layer of glycosaminoglycans [25] will limit the absorption of molecules or particulates into systemic circulation[26]. Thus, the MFH approach appears to be well-suited to concentrate heat within a MNP filled bladder, without producing hotspots in surrounding tissues.

Here, we report a preclinical thermal dosimetry analysis of the MFH approach as applied to the treatment of rat bladder, which can be easily scaled to the treatment of human bladder. We investigate the feasibility of heating rat bladder with an iron-oxide super-paramagnetic nanoparticle solution by coupling energy from an external alternating magnetic field. These results identify the major physical parameters that affect the success of heating rat bladder at 42°C, and point out some limitations of the technique.

MATERIALS AND METHODS

Animals

Twenty-five female Fisher 344 rats, 8–15 weeks old and weighing on average 161.7± 16.8 g, were purchased from Charles River Laboratories for this study. All experiments and procedures were done with the approval of the Duke University Institutional Animal Care and Use Committee. Rats were anesthetized with ketamine/xylazine (40 mg/4 mg/kg). To maintain normal body core temperature throughout the experiment, the rats were placed recumbent on a wax-pad that was regulated at approximately 38°C.

Magnetic Fluid

The magnetic fluid used in this study consisted of magnetite nanoparticles with an iron concentration of 100 mg/mL, dispersed in water (Actium Biosystems, Boulder, CO). Particles were stabilized in a water-based fluid using sodium docusate as the surfactant and proprietary methods. The mean core particle size was determined to be 20 nm using transmission electron microscopy. The composition was determined to be magnetite (Fe_3O_4) through quantitative analysis using whole X-ray diffraction pattern fitting. Magnetic characterization was performed using vibrating sample magnetometry, and the saturation magnetization of magnetite nanoparticles was determined to be approximately 400 kA/m. After successful bladder catheterization with an 18G angiocatheter, a volume of 0.4 mL of magnetic fluid was instilled into the rat bladder, and the catheter was clamped tightly. At the end of the 60 min treatment, no significant leakage of fluid was detected.

Temperature Measurements

Thermometry was carried out invasively with seven distinct fiberoptic temperature probes having a diameter of 0.42 mm (OpSens Technologies, Quebec, Quebec, Canada). Temperature probes were inserted into the vagina, rectum, and subcutaneous muscle of the upper thigh through an 18G catheter. Two temperature probes were inserted through an adjustable Port Seal (UPS-A, Gyrus Medical Ltd, Southborough, MA) mounted on the 18G bladder catheter, with one sensor carefully positioned inside the bladder and one sensor in the urethra, 8 mm proximal to the bladder. Using this monitoring configuration, body core temperature was taken as the average of the three probes located in the rectum, mouth and subcutaneous muscle sites. An additional superficial temperature measurement was recorded from a sensor on the abdominal skin surface above the bladder.

Experimental Heating protocol

Heat treatments were carried out using a small animal magnetic field applicator system (Actium Biosystems, Boulder, CO) operating at a frequency of 40 kHz and with variable field strength up to 6 kA/m. These field parameters were established for this small animal system during the system development at Actium. The control system provides two operating modes. One mode allows manual setting of desired RF magnetic field strength, and the second automatically adjusts field magnitude based on feedback control from one temperature sensor, as necessary to maintain any preset steady-state temperature (e.g., 42°C inside the bladder lumen). The magnetic field intensity was quantified during routine use of the system based on current measured in the induction coil. Calibration of the coil current to magnetic field strength was performed initially at Actium using a magnetic field probe in conjunction with a spectrum analyzer. Hyperthermia treatments were performed without any cooling system.

To test the influence of the magnetic field on non-specific heating, we conducted a control experiment with a volume of 0.4 mL of saline instilled into the rat bladder. Because initial tests indicated that air temperature inside the small rat chamber increased several degrees over a 60min treatment, this experiment was repeated under two conditions. The rats were exposed to a 5.3 kA/m field for one hour without any control of environmental temperature

around the rat. For the second condition, after one hour we added a constant flow of room temperature air through the induction coil chamber to cool the air around the rat.

Power deposition with magnetic nanoparticles

The specific loss power (SLP) is defined as the amount of energy converted into heat per time and mass of magnetic material. To evaluate the SLP, measurements of temperature rise as a function of time were carried out for various nanoparticle concentrations and applied field strengths. All magnetic fluid samples consisted of 0.4 mL of solution in 1.5 mL vial. These vials were placed in the center of the induction coil of the Actium applicator within a 3 cm thick block of Styrofoam insulation. The SLP values were calculated as,

$$SLP = c_s \frac{ms}{m_{NP}} \left(\frac{\Delta T}{\Delta t} \right) \quad (1)$$

where "c_s" is the specific heat capacity of the sample (J/g/K), "m_s" is the sample mass, "m_{NP}" is the mass of the nanoparticle in the sample (g), and ΔT/Δt is the initial 30 s slope of temperature rise versus time curve. The sample specific heat capacity (c_s) was calculated as the mass weighted mean value of the heat capacities of water and magnetite (C_{water}= 4.184 J g^{-1} K^{-1}, $C_{magnetite}$ = 0.670 J g^{-1} K^{-1}).

Power dissipation in ferrofluid in an alternating magnetic field can be described as a function of the magnetic field properties (amplitude and frequency). The widely accepted model for power dissipation in ferrofluids has been described by Rosensweig [27] and may be formulated as:

$$P = \mu_0 \pi \chi'' f H^2 \quad (2)$$

where μ_0 is the permeability of free space, χ'' is the AC magnetic susceptibility, f is the frequency of the applied AC magnetic field, and H is the strength of the applied alternating magnetic field (AC) magnetic field.

MRI measurements

For detection of magnetic nanoparticles in the bladder lumen, we acquired images with a 7T small animal MRI system (Bruker Biospec, Bruker BioSpin MRI GmbH, Ettlingen, Germany) located in the Duke Center for In Vivo Microscopy. During MR scanning, the rats were maintained under anesthesia with 1–2% isoflurane. We performed a three-dimensional, short echo-time, radial-encoding imaging sequence that acquired 134,526 views from the center of Fourier Space and uniformly sampled the periphery uniformly. The echo-time was 20 μs and the repetition time was 8.7 ms. The flip angle was 6 degrees, the field-of-view was 7 cm in all three directions, and the bandwidth was 100 kHz. Data were regridded onto a 256 x 256 x 256 matrix. The signal from fat was suppressed, and gating was not used over the total acquisition time of 20 minutes. Because MRI cannot be used with high concentration nanoparticle solutions due to excessive MR signal artifacts in surrounding tissue, a low concentration 0.5 mg/mL magnetite solution was prepared for bladder imaging.

MRI reflux detection

To determine the fluid volume required to produce vesicoureteral reflux in rats, we performed an MRI study in three rats with injected volumes ranging from 0.2 mL to 0.7 mL. Imaging of the bladder and kidneys was enhanced with injection of Gd-DTPA (Magnevist; Bayer HealthCare Pharmaceuticals, Wayne, NJ). MR images were acquired using a multi-slice gradient echo (200 frequency encoding steps, 200 phase encoding steps, 86 slices). The echo time was 4.6 ms, and the repetition time was 1.24 s. The flip angle was 90 degrees with a bandwidth of 50 kHz. The field-of-view was 7 cm in both in-plane directions, and the slice thickness was 0.35 mm. The signal from fat was suppressed, and an acquisition time of 4 minutes was used with no gating.

Based on thresholding segmentation methods, the presence of vesicoureteral reflux was detected by monitoring contrast enhancement in the kidneys before and after injection of Gd-DTPA. An initial baseline scan was performed for all rats. The bladder and kidneys were defined by manual contouring, and the organ volumes were computed. A screen of the voxel intensity distribution was performed, and the highest voxel intensity was used as a threshold value. The rats were given sequential volume injections of Gd-DTPA into the bladder, and contrast signal enhancement was computed for both kidney volumes.

RESULTS

In MFH, the key considerations are the properties of the MNP and the local environment. The process of heat dissipation in tissue during MFH involves a large set of variables. However, for a given therapeutic application, the number of variables is reduced once an appropriate ferrofluid has been established. For a given local concentration of ferrofluid in the target volume, control of therapy relies primarily on three parameters: magnetic field amplitude, magnetic field frequency, and local nanoparticle mass. In the following sections, we characterize the effects of field strength and nanoparticle concentration on our ability to heat rat bladder.

Heat dissipation characteristics of magnetic nanoparticles

Effective treatment planning and real-time control of tissue temperature need a reasonable mathematical description of power deposition in tissue. The Rosensweig description [27] is a widely accepted model to describe power deposition from MFH, within its limited range of validity [28, 29]. As is well known, the relationship between magnetic field strength (kA/m) and power deposition depends on the type of magnetic fluid [28]; therefore, our goal in this step is to verify if our system operates within the region where the Rosensweig description is valid.

First, the temperature rise, and consequently SLP, of the Actium Biosystems magnetic fluid was measured *in-vitro* for a range of applied magnetic field strengths. Figure 2 shows estimated SLP values as a function of magnetic field amplitude in vials with fixed nanoparticle volume (0.4 mL) and fixed field frequency (40 kHz).

As shown in Figure 2, we calculated a SLP of 5.6 W/g for this magnetic nanoparticle at 5.5 kA/m. The dependence of SLP with magnetic field is a reasonable fit (R^2=0.98) with the

square law, $P = \alpha f H^2$ (where α is a constant), in agreement with the Rosensweig description. Thus, the result indicates that increasing magnetic field amplitudes can systematically improve the SLP values up to 6.0 kA/m.

Catheterization feasibility

Typically, one of the primary limitations of magnetic nanoparticle therapy is the difficulty in dispersing nanoparticles uniformly throughout the target volume. For MFH applied to the bladder, the technique readily allows delivery of nanoparticles in close contact with the entire bladder wall target tissue via a single, minimally invasive catheterization procedure. In this section, we validate our ability to fill the rat bladder lumen with magnetic fluid and verify the relationship between injected volume and volume remaining in the bladder.

The nanoparticles reduce the local voxel intensity as a result of shortening the transverse relaxation times of the protons, and the bladder area containing nanoparticles appears gray. From detailed analyses of these images, it is possible to quantify the total volume of distended bladder. There was good correlation of injected volume with volume remaining in bladder for the entire 60 min heat treatment interval, showing only minor dilution from urine and no significant tissue absorption or leakage over that time period.

Non-specific heating outside the bladder

In order to identify any possible non-specific heating from eddy currents generated in the rat directly from the field, we exposed two control rats to an alternating magnetic field of amplitude 5.3 kA/m for 1 hour without injected magnetic fluid. To maintain normothermic body temperature, rats were placed on a 36–37°C pad at time of anesthesia and during treatment. Figure 4 presents the temperature trends in six different monitoring sites during the magnetic field exposure.

The temperature trends in Figure 4 show that temperature inside the coil/chamber rose 4.5°C over the first 60 min of exposure without air cooling, most likely due to joule heating of the induction coil wire. This general warming of the environment produced a corresponding increase in body core temperature, as evidenced in all monitored sites, with the highest temperature rise on the skin surface due to contact with slowly warming air. Without nanoparticles, the temperature elevation in all monitored locations was small, rising just 0.4°C in bladder lumen over the 90 min heating period. Because the temperature rise was small compared to heating from nanoparticles, subsequent experiments were performed without airflow to avoid an uncontrolled variable. However, these data suggest that future systems could benefit from controlling the temperature of air around the subject. Nevertheless, our results clearly demonstrate that the applicator meets the safety requirements of minimal direct power deposition directly in rat tissue at distance from the magnetic fluid.

Rat bladder volume restrictions

Figure 5 shows the contrast-enhancement analysis results performed in both left and right kidneys of one rat over a range of injected volumes. The increase in total signal intensity in the kidney indicates the induction of vesicoureteral reflux.

These data show that reflux into the kidneys increases dramatically when the injected volume is greater than 0.4 mL. Interestingly, the reflux was asymmetric between the two kidneys, a behavior that was observed in all rats. This is consistent with humans who develop reflux, often primarily to one kidney. The data in Figure 5 clearly underscore the need to limit injected volume to 0.35–0.4 mL for safe MFH treatment of the rat bladder.

Power deposition control

The temperature elevation in MFH depends on the local concentration of iron nanoparticles. Most applications of MFH attempt to control power deposition by modifying the number of direct injections of highly concentrated magnetic particles in the target region. In MFH of the bladder, only a single injection is required to distribute magnetic particles over the entire bladder wall target. Therefore, our approach to control power deposition in the bladder requires control of both the total fluid volume injected and the concentration of magnetic nanoparticles in the fluid. As the MRI results established a limitation of 0.4 mL for an injected volume to avoid reflux to the kidneys, we investigated our ability to adjust heat generation with a series of *in-vivo* experiments using 0.4 mL of magnetic fluid at concentrations ranging from 25 to 100 mg/mL.

Figure 6a presents representative temperature rise curves for the first 25 min of heating with 0.4 mL of magnetite nanoparticles injected into the bladder at 4 concentrations. The first 6 minutes were used to monitor the baseline temperature of the subject body. During that period we recorded all temperature values without application of magnetic field (field zero), and then the magnetic field was ramped up to the maximum set value after this initial period of monitoring.The data shown in Figure 6b indicate the min/max range of temperatures achieved after 15 min of heating as a function of concentration of injected nanoparticles (n = at least 3/data points). The data clearly demonstrate the ability of this system to heat rat bladder lumen rapidly and reliably to the desired 42°C setpoint when using a nanoparticle concentration of 100 mg/mL. Similarly, Figure 7 investigates the effect of varying the injected volume (0.2, 0.3, and 0.4 mL) of 100 mg/mL nanoparticle solution on the ability to heat rat bladder. As expected, Figure 7a indicates that the largest heat dissipation occurred for the 0.4 mL volume of magnetic fluid nanoparticles. In that case, temperatures rose quickly to the feedback control setpoint where the magnetic field was automatically reduced to maintain 42°C for the remainder of the experiment. As seen in both Figure 6a and 7a, the magnetic field was ramped up quickly only after the 6-minute period of monitoring initial conditions.

Magnetic Field Control

Control of target temperature during hyperthermia treatment is a key concern for any heating approach, and for many techniques power deposition patterns are difficult to control in heterogeneous *in vivo* tissue. In this section, we consider the quality and safety of the magnetic field control algorithm included in the Actium Biosystems induction heating system. During each heat experiment, the magnetic field amplitude was automatically controlled by a feedback control algorithm which used the temperature measured inside bladder lumen as a control signal. The goal was to maintain a constant treatment temperature of 42°C. Rapid high resolution control is important to deposit the desired thermal dose

throughout the bladder target. Figure 8 illustrates the time-dependent magnetic field amplitude required to maintain the goal treatment temperature of 42°C during a typical rat bladder treatment performed in the automatic field amplitude control mode.

The goal temperature of 42°C was reached in all animals tested with 100 mg/mL MNP. For most treatments, the steady-state temperature was maintained with magnetic field amplitudes between 3.5 and 4.5 kA/m. As depicted in the figure, the temperature inside the bladder lumen was easily maintained at 42°C by the control system during the entire period of MFH treatment.

Temperature control

Thermotherapy treatments were repeated in five rats to evaluate the ability of the control system to maintain the desired setpoint temperature in the bladder target with a safe distribution of temperatures in non-targeted tissues. All rats were injected with 0.4 mL of magnetic fluid in the bladder and placed in the field for 70 min. The control system was operated in automatic field mode, which varied magnetic field amplitude as required (up to 6 kA/m) to maintain bladder lumen temperature constant at the 42°C setpoint. Figure 9 shows average temperatures measured in bladder, vagina, and a multi-site core temperature surrogate during MFH treatments in five rats. The vertical error bars represent standard deviation of the mean temperatures. In Figure 9, the magnetic field was ramped up immediately at 0 time.

The average exposure time required to reach the goal temperature was less than 10 min. During the 60 min hyperthermia treatment, body temperature increased only 1.0–1.5°C in the absence of a cooling system. The feedback control algorithm was able to keep the temperature variation within the bladder target (red curve) to less than 0.2°C. After 60 min at 42°C, the magnetic field was switched off, and temperature dropped sharply (data not shown). Figure 9 also shows that vaginal temperatures exhibit a wider variability than other body sites. This variability may be explained by the uncertainty in probe position for the 5 animals; because the vagina is in close proximity to the bladder, this monitoring location is most sensitive to exact placement of the sensor. Despite the variation, the vaginal temperatures were clearly separated from the bladder lumen temperature measurements, demonstrating effective localization of heat within the bladder target.

The combined “body temperature” shown in Figure 9 was the average of three widely separated sites (subcutaneous, rectal, and oral sensors), which all demonstrate minimal heating during the 60 min treatment of bladder at 42°C. To provide a better sense of the complete temperature distribution throughout the rat during MFH treatment of bladder, Table I presents the steady-state temperatures measured at all seven monitored locations in the five rats.

As provided in Table I, all surrounding normal tissues were kept below 40°C at steady state, while the bladder lumen was maintained at 42°C. These results clearly demonstrate the ability to localize thermal energy dissipation within the bladder using the MFH approach.

DISCUSSION

For clinical hyperthermia applications, it is crucial to accurately control temperature in and around the target volume. Factors, such as nanoparticle size, structure, coating, concentration, local viscosity, magnetic field amplitude and frequency, play key roles in determining the power deposition in magnetic fluids. Tissue temperature rise is also highly dependent on tissue properties, such as blood perfusion cooling and homogeneous dispersion of magnetic nanoparticles within the target tissue. Although there are differences in the heating characteristics of magnetic fluids used *in vitro* versus *in vivo,* the SLP measured *in vitro* provides a reasonable metric to compare performance of different magnetic nanoparticles. *In vitro* experiments performed of magnetic fluid are the traditional method to estimate the heating potential of nanoparticles. The square law dependence of SLP on field amplitude (Figure 2) up to 5.5 kA/m indicates agreement with linear response theory; and therefore, the susceptibility may be assumed to be independent of field amplitude.

The primary goal of this study was to determine the ability of MFH to overcome limitations of other bladder hyperthermia approaches, specifically we were concerned with homogenous distribution of power deposition within the bladder target. The MRI results (provided in Figure 3) demonstrate that a homogenous distribution of magnetic fluid throughout the bladder is readily achieved via simple injection of nanoparticles through a bladder catheter. The catheterization procedure was well tolerated in rats, and placement of a Foley catheter into bladder is a standard and well-tolerated urologic procedure in humans.

One of the main criterions for hyperthermia treatment optimization is to establish the minimum amount of power required to produce a therapeutic temperature distribution in the target, allowing for efficient and preferential tumor treatment. Using the MFH technique, local power deposition is defined primarily by three parameters: magnetic field amplitude, field frequency, and local mass of magnetic nanoparticles. The amplitude and frequency field characteristics are constrained by potential patient discomfort from power deposition in tissues outside the tumor target, and total mass of magnetic nanoparticles in the target is limited by normal tissue toxicity and the ability to localize nanoparticles in the target. There are many studies that focus on toxicity of magnetite-based nanoparticles [30, 31] and thus biocompatibility was not addressed in this study. Ideally, to minimize toxicity of the particles themselves the lowest concentration of magnetic fluid necessary to produce effective heating of the target would be optimal. From the heating trial data shown in Figure 6, we identified an optimal magnetite-based iron oxide nanoparticle concentration of around 100 mg/mL for heating the 0.4 mL rat bladder. Although the target volume is much smaller, these results are consistent with the concentration used for clinical MFH treatments of human intracranial and prostate tumors [18, 20, 21, 32].

In addition to magnetic fluid concentration, the total volume of ferrofluid solution instilled in bladder also influenced effective heating. Figure 7 shows that both the heating rate and maximum temperature achieved in bladder lumen increases with increasing volume of nanoparticles. The variation in instilled volume not only changes the total mass of magnetic particles in the bladder, but also modifies heat exchange to the bladder wall and surrounding

tissue, since the ratio of nanoparticle volume to bladder wall surface area also changes. Thus, small volumes of nanoparticles with a higher concentration of particles in direct contact with perfused tissue tend to have higher thermal conduction losses into the cooler tissue. In contrast, larger volumes of nanoparticles in the bladder will attain higher temperature with the same power absorption rate, because there are more particles producing heat centrally in the bladder lumen with no contact to cooler perfused tissue. These results are in agreement with Hergt et al. [33] who indicated that the specific heating power needed to achieve a given temperature elevation increases dramatically with decreasing tumor size.

Another notable finding pertaining to the volume of injected nanoparticles concerns the possibility of inducing reflux to the kidneys in rats. Our goal was to ensure that the magnetic fluid injected into the bladder stays in the bladder and does not disperse to the kidneys or to any other normal tissue, as this could increase toxicity of the treatment. The MRI data, summarized in Figure 5, demonstrates that excessive fluid pressure in the bladder promotes reflux in rats. We determined that an upper limit of 0.4 mL of magnetic fluid could be injected to avoid redistribution of nanoparticles outside the bladder target. The possibility of reflux in rats described previously by Vercesi et. al. [34] supports our results. For future MFH studies conducted in the rat bladder, a limit of 0.35–0.4 mL injected volume should be followed to avoid unintended distribution of nanoparticles throughout the body. Reflux is not anticipated to be an issue for thermochemotherapy treatment of the human bladder. Although vesicoureteral reflux is known to occur in adult humans, its incidence is quite low (<1%) [35]. Because the bladder is generally treated after insertion of only 40 ml of drug (plus nanoparticles), that is only 10–20% of typical adult bladder capacity [35].

A principal concern for applying this methodology to human subjects is safety of the patient to the magnetic field exposure. In addition to heating magnetic nanoparticles, an alternating magnetic field generates heat directly in biological tissue by joule heat dissipation from eddy currents. This non-specific heating is directly proportional to tissue electrical conductivity and to the square of the product of magnetic field strength, frequency, and radius of eddy current loops in tissue [22, 23, 36]. The Actium Biosystems magnetic field applicator is configured to achieve magnetic field amplitudes up to 6 kA/m at 40 kHz. Based on previous work, we expect the tolerable field for non-specific heating in rats should be much higher than this field strength at 40 KHz, as rats have smaller body cross-section than humans [37]. As depicted in Figure 4, the maximum 5.3 kA/m field strength did not induce significant non-specific temperature elevation in the small diameter rat tissues. Moreover, at this operating frequency, a 6 kA/m field strength should be well within patient tolerance for continuous mode magnetic fields in the human pelvis [22, 32].

The magnetic field control study shown in Figure 8 demonstrated the effectiveness of the automatic feedback control algorithm to maintain constant temperature in the bladder lumen for the desired treatment time. In our studies, we used only one reference sensor to control the field, but for human application the easy access to the bladder allows for the use of multiple sensors that could improve the quality of the feedback signal.

Temperature sensors were placed in six normal tissue locations throughout the rat, including subcutaneous tissues at largest radius of eddy current loops from the field and in deep tissue

locations. As shown in Figure 9 and Table I, the data from these six probes provide a comprehensive sampling of rat body temperatures attained during MFH treatment. The minimum difference of 2°C between bladder lumen and all other tissues demonstrates the ability to localize heating in the desired bladder target, with little thermal conduction into nearby tissue and minimal systemic heating. In summary, bladder treatment with MFH is feasible and offers several advantages over other bladder heating approaches.

CONCLUSION

This work investigated for the first time the feasibility of applying magnetic fluid hyperthermia for heating the bladder. Using a 40 kHz induction heating system, we were able to locally heat rat bladders following injection of magnetite-based nanoparticles. Additionally, we optimized a reliable catheterization procedure that can fill the rat bladder with nanoparticles via a single injection and maintain that volume for a 60 min treatment period. We identified an injected volume limit of 0.35–0.4 mL in the rat bladder to avoid reflux to the kidneys. Bladder lumen temperatures were consistently raised to the desired 42°C in ≤ 10 min with 100 mg/mL magnetite-based nanoparticles, and this temperature was maintained by feedback control for the desired treatment time. This study demonstrated successful well-localized heating of rat bladder with MFH, with minimal systemic heating or in surrounding normal tissues. Further experiments with this procedure are warranted to investigate the efficacy and survival benefit of MFH treatments for bladder cancer.

Acknowledgments

This effort was supported by a research contract from Actium Biosystems, Boulder, CO. The authors would like to acknowledge the efforts of the entire research team at Actium in developing the small animal magnetic induction heating system and the nanoparticles used in this project. The authors appreciate the excellent support for this project from Melissa Hall.

References

1. Issels RD. Hyperthermia adds to chemotherapy. Eur J Cancer. 2008; 44(17):2546–54. [PubMed: 18789678]
2. van der Zee J. Heating the patient: a promising approach? Ann Oncol. 2002; 13(8):1173–84. [PubMed: 12181239]
3. Vujaskovic Z, Kim DW, Jones E, Lan L, Mccall L, Dewhirst MW, et al. A phase I/II study of neoadjuvant liposomal doxorubicin, paclitaxel, and hyperthermia in locally advanced breast cancer. Int J Hyperther. 2010; 26(5):514–21.
4. Kaufman DS, Shipley WU, Feldman AS. Bladder cancer. Lancet. 2009; 374(9685):239–49. [PubMed: 19520422]
5. Edge SB, Compton CC. The American Joint Committee on Cancer: the 7th edition of the AJCC cancer staging manual and the future of TNM. Ann Surg Oncol. 2010; 17(6):1471–4. [PubMed: 20180029]
6. Peichl M, Dill S, Jirousek M, Suess H. Passive microwave remote sensing for security applications. Europ Radar Conf. 2007:32–5.
7. Malmstrom PU, Sylvester RJ, Crawford DE, Friedrich M, Krege S, Rintala E, et al. An individual patient data meta-analysis of the long-term outcome of randomised studies comparing intravesical mitomycin C versus bacillus Calmette-Guerin for non-muscle-invasive bladder cancer. Eur Urol. 2009; 56(2):247–56. [PubMed: 19409692]

8. Sugiura T, Hirata H, Hand JW, Van Leeuwen JMJ, Mizushina S. Five-band microwave radiometer system for noninvasive brain temperature measurement in newborn babies: Phantom experiment and confidence interval. Radio Sci. 2011:46.
9. Tognolatti P, Giusto R, Bardati F. A new multifrequency microwave radiometer for medical operation. Sensor Actuat a-Phys. 1992; 32(1–3):291–6.
10. Colombo R, Da Pozzo LF, Salonia A, Rigatti P, Leib Z, Baniel J, et al. Multicentric study comparing intravesical chemotherapy alone and with local microwave hyperthermia for prophylaxis of recurrence of superficial transitional cell carcinoma. Journal of Clinical Oncology. 2003; 21(23):4270–6. [PubMed: 14581436]
11. Gofrit ON, Shapiro A, Pode D, Sidi A, Nativ O, Leib Z, et al. Combined local bladder hyperthermia and intravesical chemotherapy for the treatment of high-grade superficial bladder cancer. Urology. 2004; 63(3):466–71. [PubMed: 15028439]
12. Jacobsen S, Klemetsen O. Active antennas in medical microwave radiometry. Electron Lett. 2007; 43(11):606–8.
13. Moskovitz B, Halachmi S, Moskovitz M, Nativ O. 10-year single-center experience of combined intravesical chemohyperthermia for nonmuscle invasive bladder cancer. Future Oncol. 2012; 8(8): 1041–9. [PubMed: 22894675]
14. Hashimoto T, Hisazumi H, Nakajima K, Matsubara F. Studies on endocrine changes induced by 8 MHz local radiofrequency hyperthermia in patients with bladder cancer. Int J Hyperthermia. 1991; 7(4):551–7. [PubMed: 1919150]
15. Kakehi M, Ueda K, Mukojima T, Hiraoka M, Seto O, Akanuma A, et al. Multi-institutional clinical studies on hyperthermia combined with radiotherapy or chemotherapy in advanced cancer of deep-seated organs. Int J Hyperther. 1990; 6(4):719–40.
16. Yuan Y, Cheng KS, Craciunescu OI, Stauffer PR, Maccarini PF, Arunachalam K, et al. Utility of treatment planning for thermochemotherapy treatment of nonmuscle invasive bladder carcinoma. Med Phys. 2012; 39(3):1170–81. [PubMed: 22380348]
17. Salahi S, Maccarini PF, Rodrigues DB, Etienne W, Landon CD, Inman BA, et al. Miniature microwave applicator for murine bladder hyperthermia studies. Int J Hyperthermia. 2012; 28(5): 456–65. [PubMed: 22690856]
18. Jordan A, Maier-Hauff K. Magnetic nanoparticles for intracranial thermotherapy. Journal of Nanoscience & Nanotechnology. 2007; 7(12):4604–6. [PubMed: 18283851]
19. Maier-Hauff K, Rothe R, Scholz R, Gneveckow U, Wust P, Thiesen B, et al. Intracranial thermotherapy using magnetic nanoparticles combined with external beam radiotherapy: results of a feasibility study on patients with glioblastoma multiforme. Journal of Neuro-Oncology. 2007; 81(1):53–60. [PubMed: 16773216]
20. Johannsen M, Thiesen B, Wust P, Jordan A. Magnetic nanoparticle hyperthermia for prostate cancer. Int J Hyperthermia. 2010; 26(8):790–5. [PubMed: 20653418]
21. Thiesen B, Jordan A. Clinical applications of magnetic nanoparticles for hyperthermia. Int J Hyperther. 2008; 24(6):467–74.
22. Atkinson WJ, Brezovich IA, Chakraborty DP. Usable frequencies in hyperthermia with thermal seeds. IEEE Trans Biomed Eng. 1984; 31(1):70–5. [PubMed: 6724612]
23. Stauffer PR, Cetas TC, Jones RC. Magnetic induction heating of ferromagnetic implants for inducing localized hyperthermia in deep seated tumors. Ieee T Bio-Med Eng. 1984; 31:235–51.
24. Stauffer PR, Sneed PK, Hashemi H, Phillips TL. Practical induction heating coil designs for clinical hyperthermia with ferromagnetic implants. Ieee T Bio-Med Eng. 1994; 41(1):17–28.
25. Tyagi P, Wu PC, Chancellor M, Yoshimura N, Huang L. Recent advances in intravesical drug/gene delivery. Mol Pharmaceut. 2006; 3(4):369–79.
26. Tyagi P, Wu PC, Chancellor M, Yoshimura N, Huang L. Recent advances in intravesical drug/gene delivery. Molecular pharmaceutics. 2006; 3(4):369–79. [PubMed: 16889430]
27. Roberts KB. Urinary tract infection: clinical practice guideline for the diagnosis and management of the initial UTI in febrile infants and children 2 to 24 months. Pediatrics. 2011; 128(3):595–610. [PubMed: 21873693]

28. Bordelon DE, Cornejo C, Gruttner C, Westphal F, DeWeese TL, Ivkov R. Magnetic nanoparticle heating efficiency reveals magneto-structural differences when characterized with wide ranging and high amplitude alternating magnetic fields. J Appl Phys. 2011; 109(12)
29. Hergt R, Dutz S, Zeisberger M. Validity limits of the Neel relaxation model of magnetic nanoparticles for hyperthermia. Nanotechnology. 2010; 21(1)
30. Lewinski N, Colvin V, Drezek R. Cytotoxicity of nanoparticles. Small. 2008; 4(1):26–49. [PubMed: 18165959]
31. Kim JS, Yoon TJ, Kim BG, Park SJ, Kim HW, Lee KH, et al. Toxicity and tissue distribution of magnetic nanoparticles in mice. Toxicol Sci. 2006; 89(1):338–47. [PubMed: 16237191]
32. Wust P, Gneveckow U, Johannsen M, Bohmer D, Henkel T, Kahmann F, et al. Magnetic nanoparticles for interstitial thermotherapy--feasibility, tolerance and achieved temperatures. Int J Hyperther. 2006; 22(8):673–85.
33. Hergt R, Dutz S. Magnetic particle hyperthermia-biophysical limitations of a visionary tumour therapy. J Magn Magn Mater. 2007; 311(1):187–92.
34. Ofek I, Goldhar J, Zafriri D, Lis H, Adar R, Sharon N. Anti-Escherichia coli adhesin activity of cranberry and blueberry juices. N Engl J Med. 1991; 324(22):1599. [PubMed: 1674106]
35. Choi YD, Yang WJ, Do SH, Kim DS, Lee HY, Kim JH. Vesicoureteral reflux in adult women with uncomplicated acute pyelonephritis. Urology. 2005; 66(1):55–8. [PubMed: 15993478]
36. Stauffer PR, Fletcher AM, DeYoung DW, Dewhirst MW, Oleson JR, Cetas TC. Observations on the use of ferromagnetic implants for inducing hyperthermia. Ieee T BioMed Eng. 1984; 31(1):76–90.
37. Ivkov R, DeNardo SJ, Daum W, Foreman AR, Goldstein RC, Nemkov VS, et al. Application of high amplitude alternating magnetic fields for heat induction of nanoparticles localized in cancer. Clin Cancer Res. 2005; 11(19):7093s–103s. [PubMed: 16203808]

Figure 1.
Induction coil chamber and power supply of a small animal magnetic field hyperthermia system (Actium Biosystems) with thermal monitoring and control console.

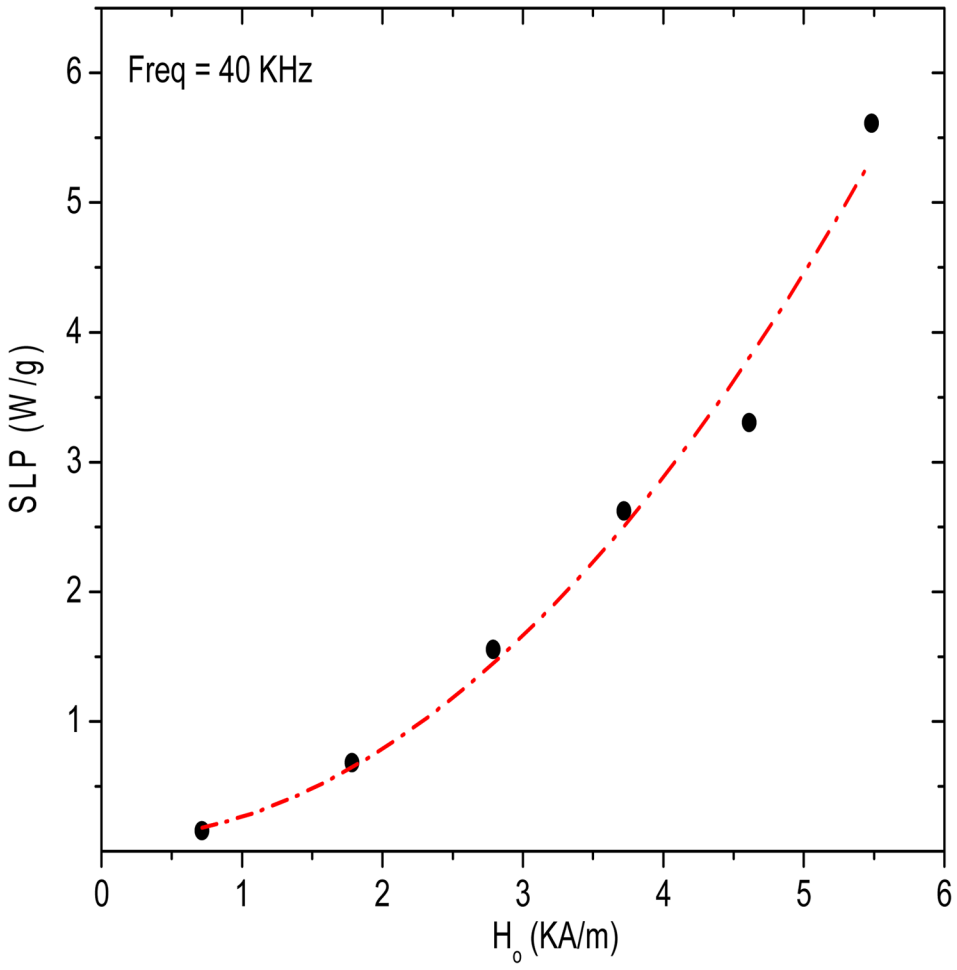

Figure 2.

Specific loss power (SLP) as a function of magnetic field strength for 0.4mL of 100 mg/mL magnetite nanoparticle solution at a fixed frequency of 40 kHz. The dashed line represents the best fit line to H^2-law ($R^2 = 0.98$).

Figure 3.
Pretreatment MRI image showing the rat bladder filled with 0.5mL of 0.5 mg/mL magnetic fluid. Arrows highlight the catheter placement through the urethra to the bladder.

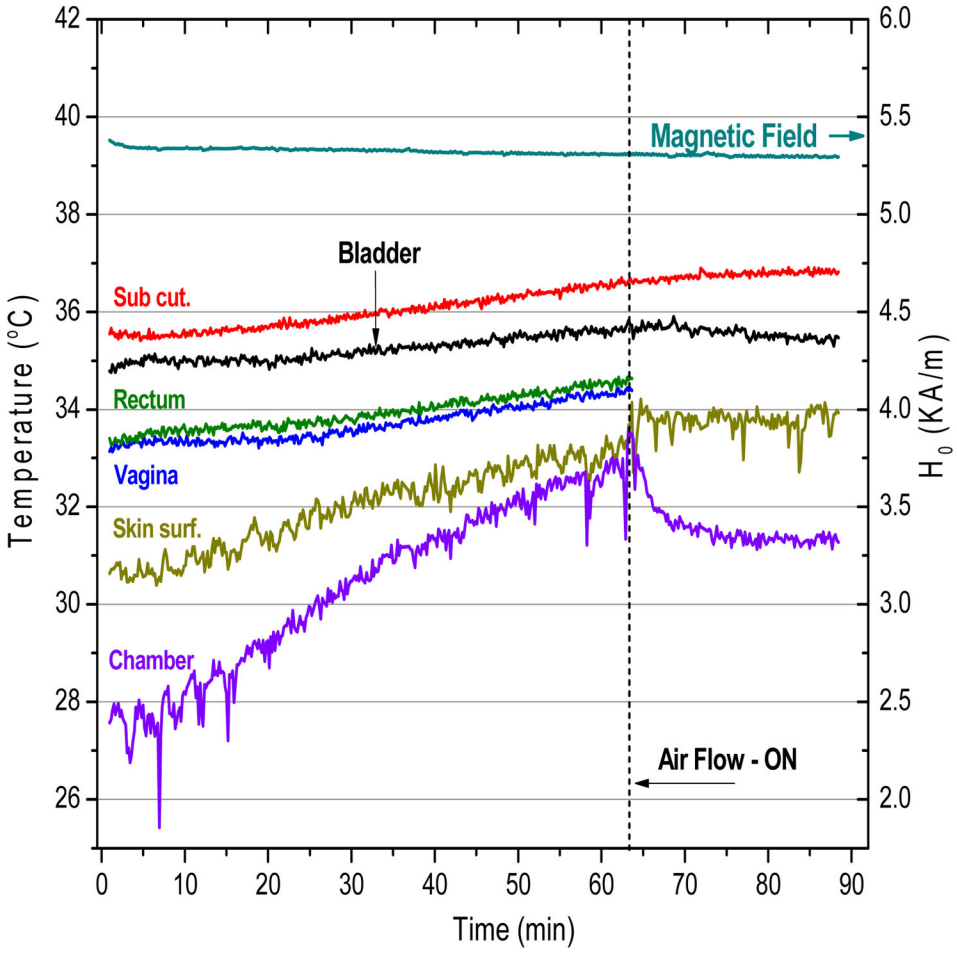

Figure 4.

Non-specific heating of rat tissues from exposure to 5.3 kA/m magnetic field at 40 kHz with 0.4mL saline instilled into the bladder. A slow temperature rise of rat tissues follows the overall increase in air temperature inside the coil.

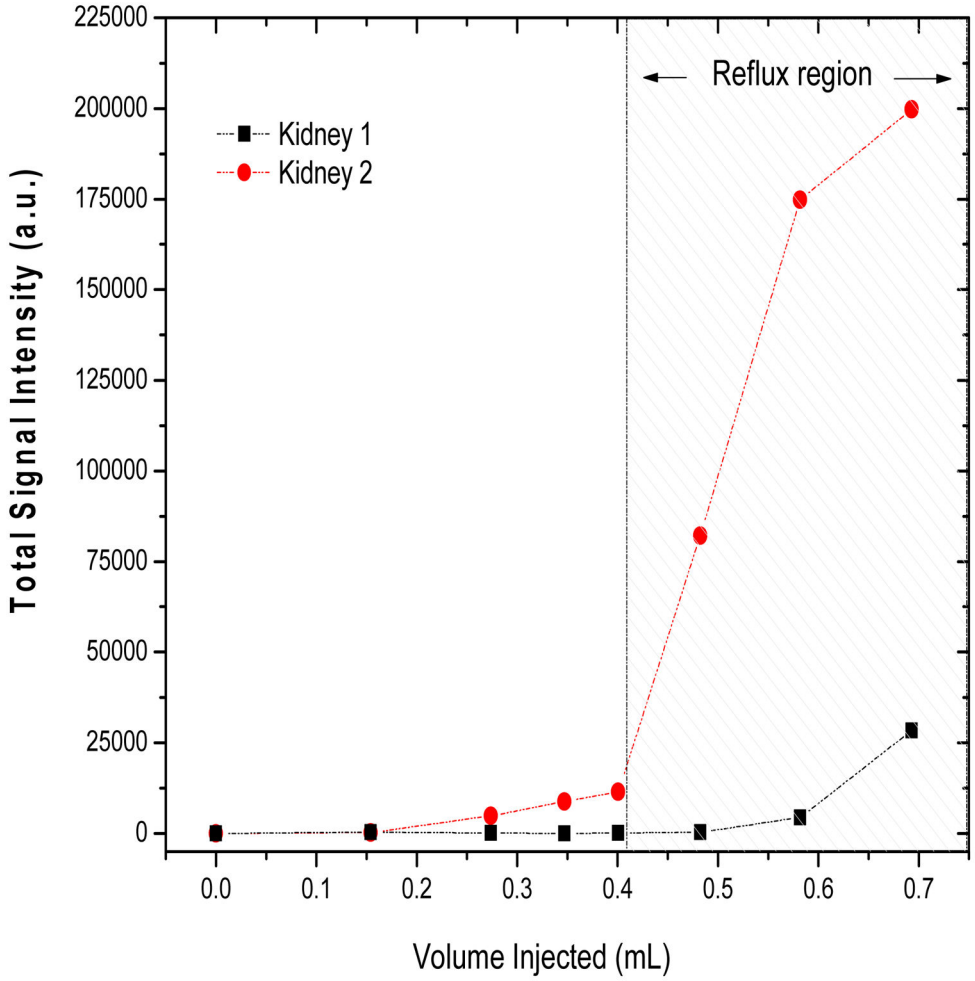

Figure 5.

Amplitude of contrast-enhacement in the kidneys as a function of Gd-DTPA volume injected into the rat bladder. The bladder volume was determined by manual segmentation of the MR images as verification of the injected volumes.

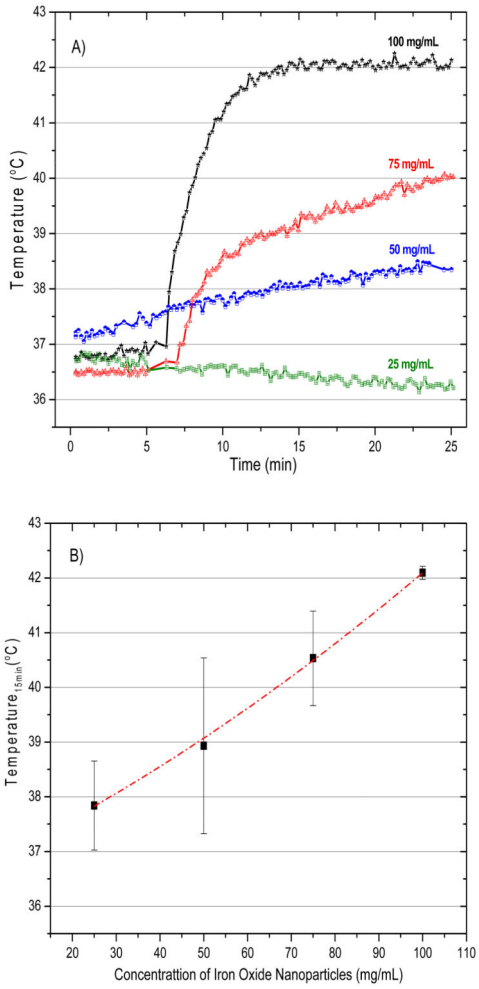

Figure 6.

Temperatures achieved inside the rat bladder following exposure to 5.5 kA/m magnetic field at 40 kHz. (A) representative heating rate profiles for four different rats injected with 0.4mL of a range of magnetite concentrations (25–100 mg/mL), and (B) bladder temperatures achieved after 15 min of heating as a function of magnetite concentration. The bars represent the maximum and minimum values obtained in at least three animals per data point.

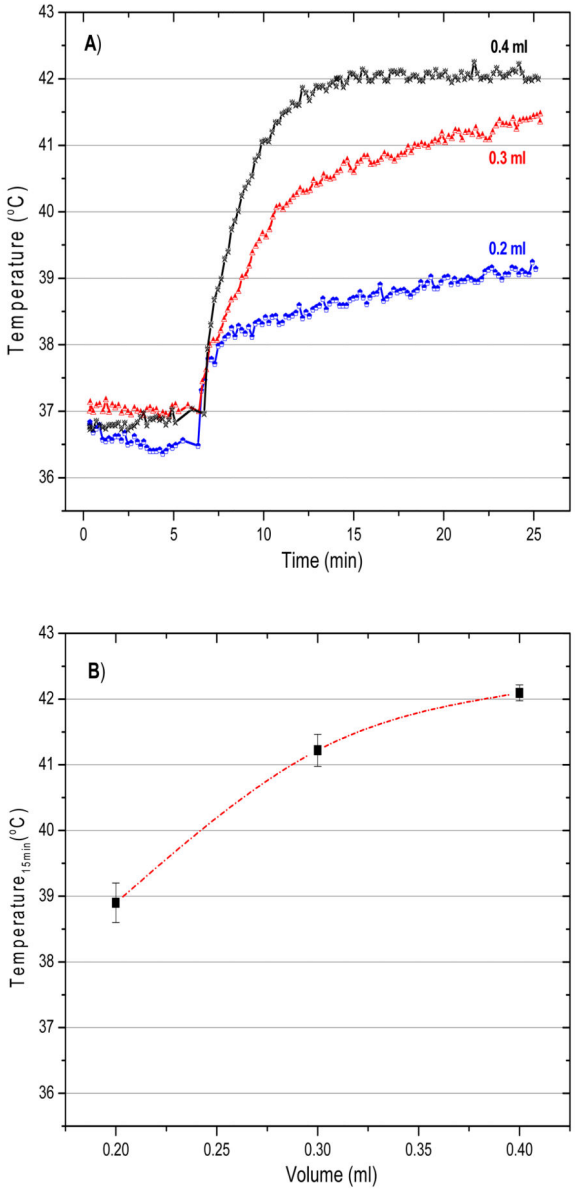

Figure 7.

Temperatures achieved inside the rat bladder after exposure to 5.5 kA/m magnetic field at 40 kHz. (A) representative heating rate profiles for three different rats injected with different volumes of 100 mg/mL magnetite nanoparticles, and (B) bladder temperatures achieved after 15 min of heating as a function of injected volume. The bars represent the maximum and minimum values obtained in at least three rats per data point.

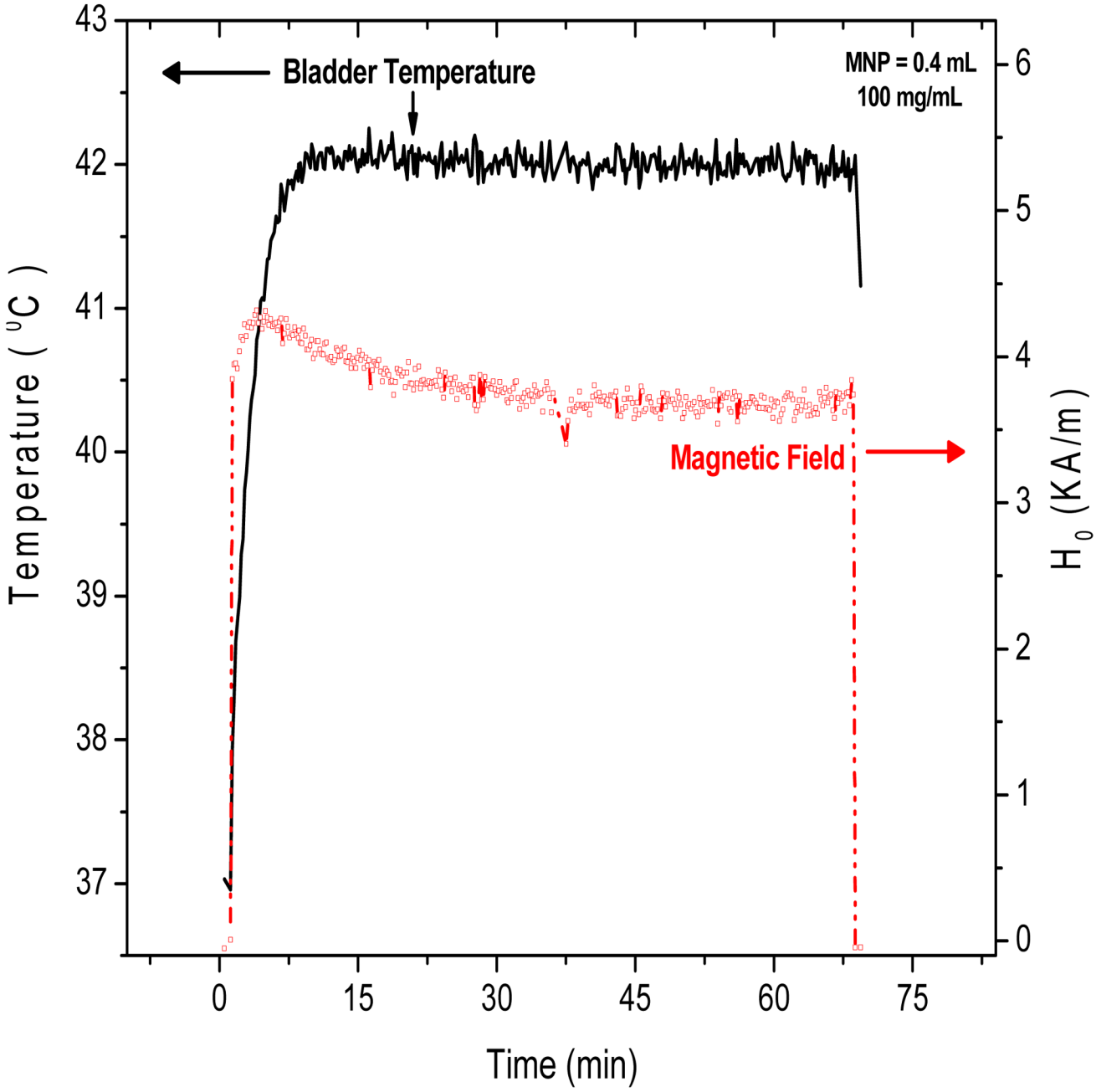

Figure 8.

Typical magnetic field amplitude (red line, right axis) applied during MFH treatment (0.4mL of 100 mg/mL nanoparticles) required to achieve the goal temperature of 42 C inside the rat bladder (black line, left axis).

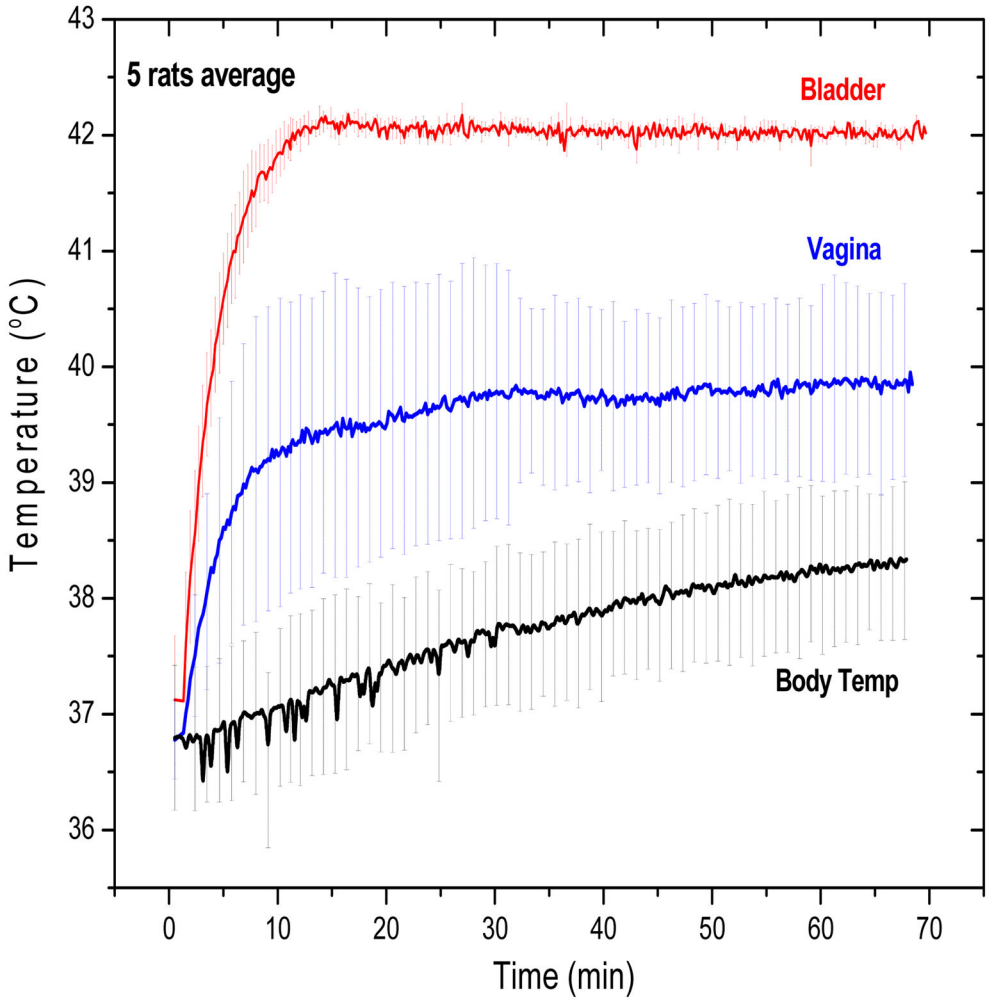

Figure 9.

Average temperature obtained in five rats during 1 h MFH treatment. Note the excellent localization of heat in the bladder target and lower temperatures in surrounding normal tissues such as the vagina (blue) and other body sites (black). The ‘body temperature’ curve (black) represents the average of measurements from subcutaneous, rectal and oral probes which were similarly low compared to the bladder temperature. The nanoparticle concentration for all treatments was 100 mg/mL..

Table I

Steady state temperatures achieved at all monitored sites in five rats heated to 42 o C in bladder (with standard deviations in parentheses).

	Environment	Subcutaneous	Bladder	Urethra	Vagina	Rectum	Mouth
Temperature (°C)	31 (2)	38.1 (0.8)	42.0 (0.2)	39.6 (0.8)	39.8 (0.8)	38.3 (0.7)	37.6 (0.8)